Extraction of dispersion surfaces: a review of applications, methods and open questions

Pierre Margerit

Extraction of dispersion surfaces: a review of applications, methods and open questions

Pierre Margerit [1]
[1] PIMM Laboratory, UMR CNRS 8006, ENSAM Paris,
151 bd. de l'Hôpital, 75013 Paris
e-mail: **pierre.margerit@ensam.eu**

Abstract
The use of dispersion surfaces to describe the wave propagation characteristics of a structure is motivated using experimental data. A review of the different approaches allowing for a high-resolution estimation of the wave parameters from a full-field measurement is given. The sensitivity of each method with regard to measurement noise and model bias is compared throughout numerical examples.

1 Introduction

The development of dynamical full-field measurement techniques [1] opens the door for the formulation of original structural identification procedures using the rich data available [2]. More precisely, these new wide-band methods aim to bridge the gap between modal analysis [3] and ultrasound techniques [4], respectively confined to the low and high ends of the frequency spectrum. In addition, a particular effort is dedicated to inverse methods with formulations that are insensitive to boundary conditions and applied loads in order to open the door to *in-situ* implementations. Indeed, such methods focus on the characterization of the transfer mechanisms in the structure of interest, represented by its governing equations of motion, or, equivalently, its wave propagation characteristics.

The *linear* equations of *free harmonic* motion of any *macroscopically invariant* structure can be expressed in the form of a *differential* system of homogeneous equations $\mathscr{L}\big(\underline{\boldsymbol{u}}, \{p_i\}\big) = 0$, where $\underline{\boldsymbol{u}}(\underline{\boldsymbol{x}})$ is a kinematic field (e.g generalized displacement or velocity), $\underline{\boldsymbol{x}}$ the spatial coordinate and $\{p_i\}$ is a set of coefficients sampling the structural *viscoelastic* behavior. The robust estimation $\{\widetilde{p}_i\}$ from a partial and noisy measurement $\widetilde{\underline{\boldsymbol{u}}}$ remains an active field of research in different communities ranging from (multidimensionnal) system identification to (architectured) material characterization.

Two main approaches may be identified in the litterature: (i) direct minimization of the residual $\mathscr{L}\big(\widetilde{\underline{\boldsymbol{u}}}, \{\widetilde{p}_i\}\big)$, using either finite difference schemes (e.g Force Analysis Technique [5, 6, 7]) or a weak formulation (e.g Virtual Fields Method [8, 9]); (ii) decomposition of the measured field $\widetilde{\underline{\boldsymbol{u}}}$ on a set of *elementary* solutions $\underline{\boldsymbol{u}}_e(\underline{\boldsymbol{x}})$ of the operator $\mathscr{L}$, using for example Green functions [10, 11] or plane waves [12, 13, 14, 15, 16, 17, 18].

The first approach provides a direct relation between the measured data and the parameters to be identified and can be generally applied to a wide range of operators. However, the full kinematics of the structure have to be measured, thus reducing the application to simple models (e.g thin plates or beams). In addition, high-order derivatives have to be estimated (e.g fourth-order for the bending motion), leading to a relative sensitivity of the identified parameters to measurement noise.

By contrast, the second approach using elementary solutions of the operator overcome the observability limitation, as only the *projection* of these solutions on a *partially observed* kinematic field is needed. However, the dependence of these solutions as a function of the parameters $\boldsymbol{p}$ is not direct, especially in the case of Green functions that are known analytically in very few situations (e.g elliptical orthotropy for thin plates).

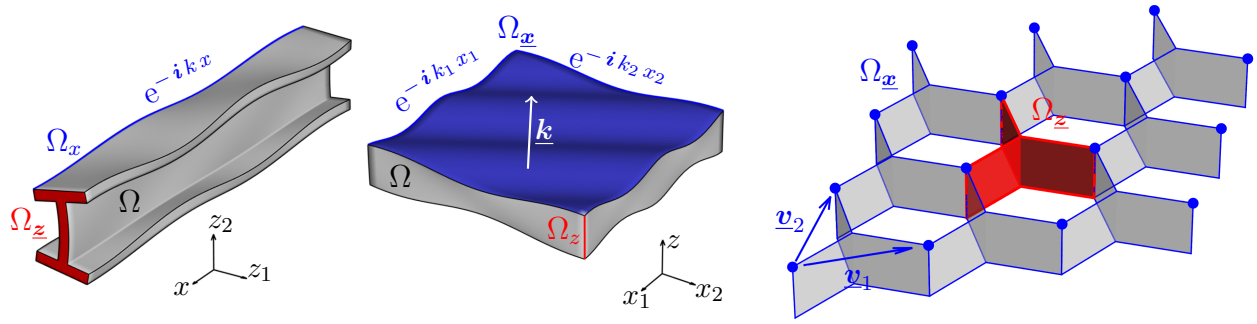

(a) Beam

(b) Plate

(c) Periodic honeycomb

Figure 1: Typical waveguides

Similarly, using plane waves $\underline{\boldsymbol{u}}_e = \underline{\boldsymbol{a}} \exp(-\boldsymbol{i}\, \underline{\boldsymbol{k}} \cdot \underline{\boldsymbol{x}})$ as the field approximation basis, the parameters $\boldsymbol{p}$ are related to the wavevectors $\underline{\boldsymbol{k}}$ via the *dispersion* relations associated to $\mathscr{L}$, which analytical expressions are only available for a very limited range of structures.

However, the approximation of a measured field with plane waves does not require *a priori* knowledge of the underlying operator, thus providing a very general framework for the identification of the system dispersion characteristics. This is of particular interest when the behavior of the structure of interest is not known, and may be viewed as an *intermediate* step in the identification process.

2 Dispersion surfaces

Plane wave propagation is associated to the formalism of *wave guides*, that are characterized by a *characteristic microstructure* $\Omega_{\underline{\boldsymbol{z}}}$ that is *tiled* over a macroscopic domain $\Omega_{\underline{\boldsymbol{x}}}$ such that the full structural domain can be expressed as $\Omega = \Omega_{\underline{\boldsymbol{z}}} \otimes \Omega_{\underline{\boldsymbol{x}}}$ (see the figure 1):

- *Homogeneous waveguides* with a charateristic *section* $\Omega_{\underline{\boldsymbol{z}}}$
- *Periodic waveguides* with a *unit cell* $\Omega_{\underline{\boldsymbol{z}}}$ tiled with periodicity vectors $\{\underline{\boldsymbol{v}}_i\}$ such that $\underline{\boldsymbol{x}}$ and $\underline{\boldsymbol{z}}$ denote the separation of *scales* (resp. macroscopic and microscopic)

From the theoretical point of view, plane waves are generally expressed as:

$$\underline{\boldsymbol{u}}_e(\underline{\boldsymbol{x}}, \underline{\boldsymbol{z}}) = \underline{\boldsymbol{\Phi}}(\underline{\boldsymbol{z}})\ \mathrm{e}^{-\boldsymbol{i}\, \underline{\boldsymbol{k}} \cdot \underline{\boldsymbol{x}}} \tag{1}$$

where $\underline{\boldsymbol{k}}$ is the so-called *wavevector* and $\underline{\boldsymbol{\Phi}}(\underline{\boldsymbol{z}})$ the corresponding wave *mode*. Injecting the equation (1) in the differential operator $\mathscr{L}$ leads to a general expression of the dispersion equations:

$$\underline{\underline{\boldsymbol{D}}}(\underline{\boldsymbol{k}}, \omega)\, \underline{\boldsymbol{\Phi}}(\underline{\boldsymbol{z}}) = \underline{\boldsymbol{0}} \tag{2}$$

where the dependence on the frequency ω have been explicitly written in order to show that the solutions of the equation (2) form a *discrete* set of hypersurfaces in the $(\underline{\boldsymbol{k}}, \omega)$ Fourier space: the so-called *dispersion surfaces*.

Experimentally, the dispersion surfaces can be obtained by computing the frequency-wavevector spectrum as the multidimensional Discrete Fourier Transform (DFT) of the structure response measured over spatio-temporal grid of $(N_1, \ldots, N_d, N_t)$ points with uniform spacings $(\Delta x_1, \ldots, \Delta x_d, \Delta t)$, so that $L_i = N_i \Delta x_i$ and $T = N_t \Delta t$.

In the figure 2, the experimental dispersion surfaces of a Sandwich plate made of an isotropic foam core between two Carbon Fiber Reinforced Polymer (CFRP) skins are displayed. The theoretical dispersion surfaces, computed with the Spectral Finite Element Method [19], are superimposed. The different propagating wave modes are well separated: out-of-plane bending, in-plane shear and traction. Surprisingly, the signature

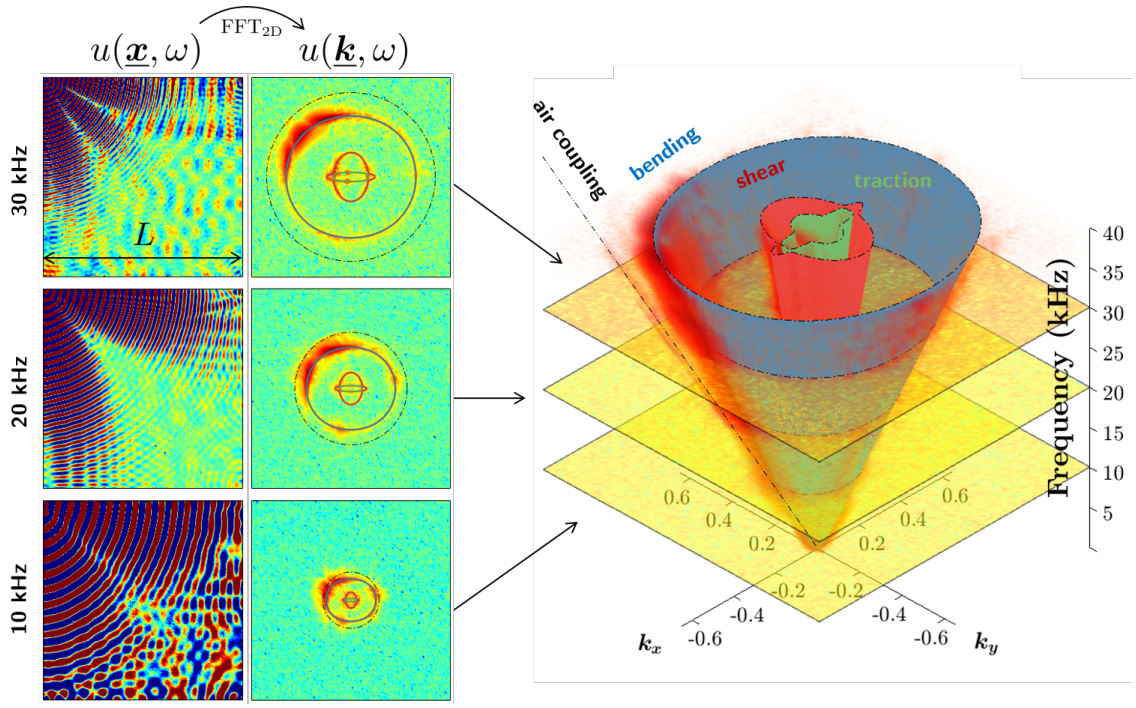

Figure 2: Dispersion surfaces associated to a sandwich CFRP plate.

of the fluid-structure interaction with the surrounding air also appears as an additional dispersion surface (see [17] for more details).

In the figure 3, the experimental spatio-temporal response of a PVC beam ($L \times S = 1\text{m} \times 15^2\text{mm}^2$, $E = 5\text{GPa}$, $G = 2\text{GPa}$, $\rho = 1380\text{kg/m}^3$) is displayed with its corresponding frequency-wavenumber spectrum. For vizualization purposes, the bending and torsion have been separated by measuring the structure response on several points over the beams width. The dispersion curves corresponding to the two motion mechanisms are well captured on the frequency-wavenumber spectrum (as hypersurfaces in a 2D domain) and show an excellent agreement with theoretical predictions (see [16] for more details).

Hence, dispersion surfaces appear as an excellent candidate for the characterization of the dynamical behavior of structures: (i) they can easily be obtained as the Fourier transform of a full-field measurement of the structure kinematics; (ii) few assumptions are involved (only the system linearity), making the approach relatively general; (iii) they can be compared to theoretical predictions of the wave dispersion (Eq. (2)) without taking into account boundary conditions or applied loads, thus providing a framework for *in-situ* identification procedures. However, the use of the Fourier transform to obtain the frequency-wavenumber spectrum is submitted to the uncertainty principle:

$$\Delta x_i \, \Delta k_i = 2\pi / N_i \tag{3}$$

which applies also to the couple (ω, t) and gives the maximum wavenumer $k_i^{\max} = 2\pi/\Delta x_i$ and the wavenumber resolution $\Delta k_i = 2\pi/L_i$. While $k_i^{\max}$ can be increased by a refinement of the measurement mesh, the wavenumber resolution Δk_i is bounded by the size of the structure of interest. This strong constraint thus motivates the development of dispersion surface extraction methods that overcome the resolution limitation.

3 Extraction methods

The development of alternatives to the Fourier transform for the extraction of dispersion surfaces is motivated by two needs: (i) overcoming the wavenumber resolution limit; (ii) allowing the extraction of the imaginary

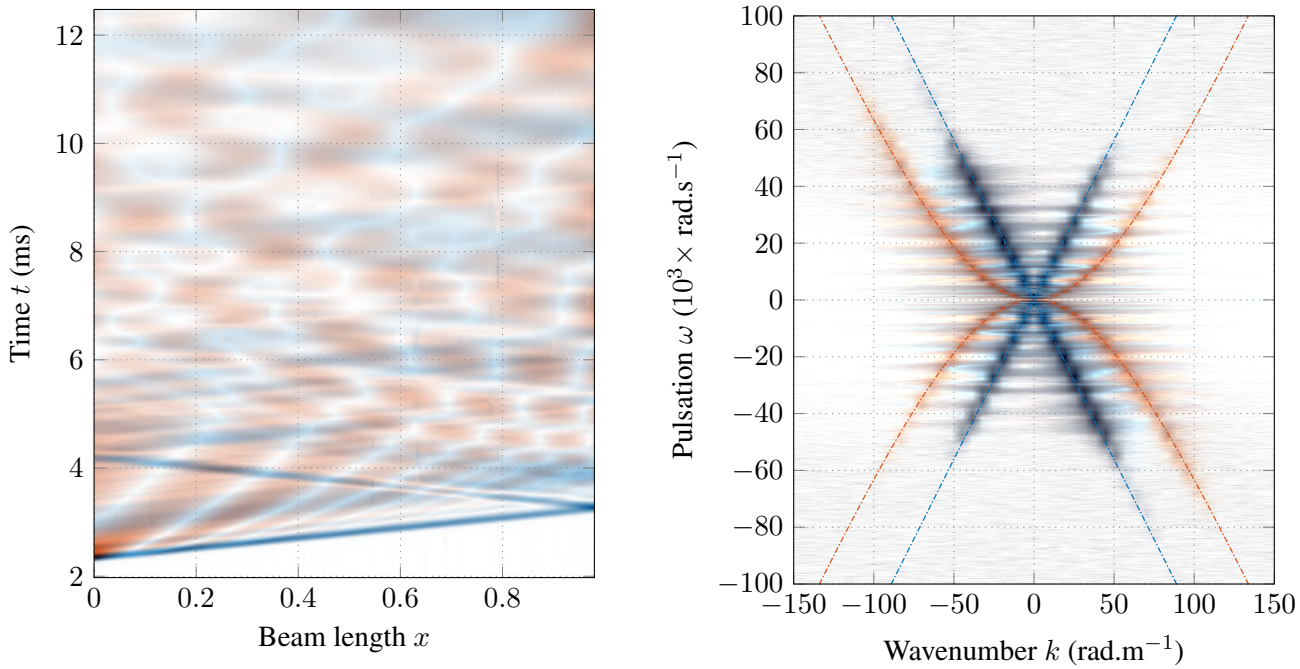

(a) Spatio-temporal signal

(b) Fourier spectrum

Figure 3: Dispersion of torsion and bending waves in an homogeneous PVC beam

part of the wavenumber that describes the attenuation of waves thus samples the viscous part of the structure behavior.

For the sake of readability, the following developments are given for the elementary case of a scalar field $u(x) \in \mathbb{C}$ measured along a unidimensional grid $\{x_n = x_0 + n\Delta x, n = 0 \dots N-1\}$ and corresponding to the harmonic response of a structure, such that the frequency ω is fixed and the waves are parameterized by a scalar wavenumber $k \in \mathbb{C}$. The generalization of the reported methods to multidimensional waves and grids is, in most of the case, relatively straightforward and is not developed here (the reader is thus referred to the given references for implementation details).

Most method formulations start with a combination of plane waves s as *signal model*:

$$s(\{a_r\}, \{k_r\}, x) = \sum_r^R a_r \exp(\boldsymbol{i}\, k_r\, x) \tag{4}$$

where the *signal order* R and the sets of wave amplitudes $\{a_r\} \in \mathbb{C}^R$ and wavenumbers $\{k_r\} \in \mathbb{C}^R$ have either to be estimated or assumed.

In the following, the review of available methods is separated into three approaches: (1) non-linear minimization, (2) low-rank approximation and (3) kernel identification procedures.

3.1 Non-linear regression

Given a signal order R, the set of wavenumbers $\{k_r\}$ can be estimated from the measured field using the following double minimization problem:

$$\left\{\widetilde{k}_r\right\} = \underset{\{k_r\}\in\mathbb{C}^R}{\arg\max} \left\{ \min_{\{a_r\}\in\mathbb{C}^R} \sum_n \left(s(\{a_r\}, \{k_r\}, x_n) - \widetilde{u}(x_n) \right)^2 \right\} \tag{5}$$

which is solved as a two-step procedure: (i) for a given set of wavenumbers, determine $\{a_r\}$ using linear least-squares; (ii) find the set $\{k_r\}$ that minimizes the error residual.

In order to reduce the complexity of this non-linear search, one can assume: (i) a unitary signal order ($R = 1$), as in the IWC [13, 14] (Inhomogeneous Wave Correlation) and the SLaTCoW [15] (Spatial LAplace Transform for COmplex Wavenumber) methods; (ii) a relation between the wavenumbers, as in the McDaniel method [20] where the four bending wavenumbers are searched simultaneously as $\{k, \boldsymbol{i}\, k, -k, -\boldsymbol{i}\, k\}$. While the latter strategy is limited to simple structures where the wavewnumber relation is known *a priori*, it is associated to an *exact* signal model thus is very robust to noise and overcome the wavenumber resolution (see [16]). This is not the case of both IWC and SLaTCoW methods, that can be regarded as the maximization of a normalized *Laplace* Transform and inherit its resolution limitations. Despite their respective limitations, these approaches are relatively simple to implement and thus are a good candidate for a first extraction of wave characteristics from a measured structure response before the application of more sophisticated methods.

3.2 Low-rank approximation

The purpose of the following family of methods is to provide: (1) a criterion to estimate the signal order R; (2) a *direct* (optimization-free) identification of the wavenumbers $\{k_r\}$.

The vector $\boldsymbol{s} = {}^{\top}[s(x_0)\ \ldots\ s(x_{N-1})] \in \mathbb{C}^N$ representing the pure signal model (4) sampled along a uniform grid of points can be rewritten as follows:

$$\boldsymbol{s} = \mathbf{V} \cdot \boldsymbol{a} \tag{6}$$

where $\mathbf{V} \in \mathbb{C}^{N \times R}$ is the so-called Vandermonde matrix with components $V_{n,r} = \exp(\boldsymbol{i}\, k_r\, x_n)$ and $\boldsymbol{a} \in \mathbb{C}^R$ contains the wave amplitudes $\{a_r\}$.

The Vandermonde matrix exhibits a so-called *rotational* or *shift* invariance between two lines -or sampling locations- such that $V_{n+1,r} = V_{n,r} \exp(\boldsymbol{i}\, k_r\, \Delta x)$, or in matrix notation:

$$\mathbf{V}_{\uparrow} = \mathbf{V}_{\downarrow} \cdot \mathbf{Z} \tag{7}$$

where $\mathbf{V}_{\uparrow}$ and $\mathbf{V}_{\downarrow}$ respectively contain the $N-1$ *last* and *first* rows of $\mathbf{V}$ and $\mathbf{Z} = \mathrm{diag}\left(\{\exp(\boldsymbol{i}\, k_r\, \Delta x)\}\right) \in \mathbb{C}^{R \times R}$ is the *pole* matrix. Hence the wavenumbers $k_r = -\boldsymbol{i} \log(Z_{r,r}) / \Delta x$ can be estimated once the Vandermonde matrix is known; which is in practice impossible.

Assuming a *low signal order* such that $R < N$, the signal $\boldsymbol{s}$ is of low rank; in particular, one can define a Hankel matrix $\mathbf{H} \in \mathbb{C}^{M \times Q}$ with components $H_{m,q} = s_{m+q}$ that is *rank-defficient* so that the following *subspace decomposition* applies:

$$\mathbf{C}_{ss} = {}^{\mathsf{H}}\mathbf{H} \cdot \mathbf{H} = {}^{\mathsf{H}}\mathbf{W} \cdot \mathrm{diag}\left(\boldsymbol{\lambda}\right) \cdot \mathbf{W} + {}^{\mathsf{H}}\mathbf{W}_{\perp} \cdot \mathrm{diag}\left(\boldsymbol{\lambda}_{\perp}\right) \cdot \mathbf{W}_{\perp} \tag{8}$$

where $\mathbf{W} \in \mathbb{C}^{Q \times R}$ is the *signal subspace* associated to non-zero eigenvalues $\boldsymbol{\lambda} \in \mathbb{C}^R$ and $\mathbf{W}_{\perp} \in \mathbb{C}^{Q \times (Q-R)}$ is an arbitrary orthogonal associated to vanishing eigenvalues $\boldsymbol{\lambda}_{\perp} \in \mathbb{C}^{(Q-R)}$. While the signal order R can be estimated by observing the number of non-zero eigenvalues, it can also be shown that $\mathbf{W}$ spans the same subspace as the Vandermonde matrix so that $\mathbf{W} = \mathbf{V} \cdot \mathbf{T}$ with $\mathbf{T} \in \mathbb{C}^{R \times R}$ a transfer matrix. Thus the pole matrix $\mathbf{Z}$ can be directly estimated from the signal subspace as the eigenvalues of the *spectral matrix* $\mathbf{F}$:

$$\mathbf{F} = \mathbf{W}_{\uparrow}{}^{\dagger} \cdot \mathbf{W}_{\downarrow} = \mathbf{T}^{-1} \cdot \mathbf{Z} \cdot \mathbf{T} \tag{9}$$

where $\mathbf{W}_{\uparrow}$ and $\mathbf{W}_{\downarrow}$ also represent shifted versions of the signal subspace and $\bullet^{\dagger}$ is the *pseudo-inverse*. An important property of the signal subspace is that it is left unchanged by an additional white gaussian noise applied to the signal. This gives the preceding approach a relative robustness with regard to experimental noise and modeling error.

While the subspace decomposition was first used in the MUSIC algorithm (MUltiple SIgnal Classification) [21] and the use of the shift invariance of the Vandermonde matrix proposed in the Matrix Pencil method [22], the ESPRIT algorithm (Estimation of Signal Parameters via Rotationnal Invariance Techniques) [23]

was the first to make use of both techniques via the equation (9). It thus represents an excellent candidate method for the direct estimation of a set of wavenumbers from a noisy measurement.

However, the ESPRIT algorithm, when applied to full-field measurement performed on a structure, suffers from the limitations associated to the signal model (4): (i) if the rank R of the signal is high; (ii) if the signal-to-noise is low; (iii) if the wavefront is not plane, for example in the case of a thin isotropic plate excited by a point source. In these situations, the signal order R might be difficult to estimate even with the variety of signal order estimation criteria that have been proposed in the literature: MDL (Minimum Description Length) [24], ESTER (ESTimation of ERror) [25], SAMOS (Subspace-based Automatic Model Order Selection) [26], among others. In addition, the non-plane wavefront geometry is associated to systematic errors on the wavenumber estimation, that is mainly concentrated on the imaginary part of k_r corresponding to the wave decay. As a consequence, in practice the precise identification of wave characteristics with ESPRIT is possible in situations where a signal model (4) with a low signal order R is a *good* approximation of the measured signal: (i) for structures with 1D propagation space -the macroscopic coordinate x- the signal model is *exact*; (ii) when their is a few number of components in a multidimensional signal (e.g if the reflections at the boundaries *select* particular wave propagation directions); (iii) in the *far-field* of a source, when the observed signal is close to a plane wave.

3.3 Spectrum relocalization

One strategy to overcome the high rank estimation problem is to *artificially* reduce the signal rank by filtering techniques. More precisely, a collection of M narrow-band-pass filters $\left\{\boldsymbol{f}^{(m)}\right\}$ can be applied to the signal in order to obtain a collection of reduced-order signals $\left\{\boldsymbol{\xi}^{(m)}\right\}$ that can be later processed by an ESPRIT algorithm with low order [27].

The new problem that arises is then the choice of the filter parameters: central wavenumber k_m, order Q. A systematic choice can be to choose the filter weights $\boldsymbol{f}^{(m)} \in \mathbb{C}^Q$ as a windowed complex exponential:

$$f_q^{(m)} = w_q \exp(\boldsymbol{i}\, k_m\, q) \tag{10}$$

with $\boldsymbol{w} \in \mathbb{R}^Q$ the window function and $k_m = 2\pi\, m/M$. Then it is easy to see that the $\boldsymbol{\xi}^{(m)} = \boldsymbol{f}^{(m)} \ast \boldsymbol{s}$ are the rows of the weighted column-wise DFT of the Hankel matrix $\mathbf{H}$:

$$\boldsymbol{\chi} = {}^{\top}[\boldsymbol{\xi}^{(1)} \ \ldots \ \boldsymbol{\xi}^{(M)}] = \mathcal{F}_1\Big[\mathbf{H} \cdot \mathrm{diag}\,(\boldsymbol{w})\Big] \tag{11}$$

which drastically reduces the computational complexity of the filtering step. Finally, the ESPRIT method can be applied to the individual rows of $\boldsymbol{\chi}$.

The equation (11) also shows that this particular choice of filters and the application of ESPRIT corresponds to the identification of the variation of the signal phase associated to each DFT bands as a function of the coordinate shift. This concept is at the basis of spectrogram reallocation methods [28], where the phase derivative is associated to a *local* frequency. Equivalently, fixing $R = 1$ when applying ESPRIT corresponds to the estimation of the *dominant* wavenumber associated to each DFT band; a kind of *spectrum relocalization* technique.

While the spectrum relocalization technique provide a systematic method to get around the signal order estimation problem, the bias associated to the approximation of non-planar wavefront geometries with plane waves is still present, preventing a precise determination of the wave attenuation characteristics. In addition, the choice of the window, necessary to lower border effects, has an effect on the signal model which is no longer exact.

3.4 Kernel-based

Taking a step back to the Prony family of methods that resulted from its pioneering works [29], it is well known that the 1D signal model in equation (4), when measured along a regular grid, satisfies a recurrence re-

lation of the form $\boldsymbol{s} * \boldsymbol{g} = \mathbf{0}$, where $\boldsymbol{g} \in \mathbb{C}^{R+1}$ is the signal kernel which coefficients define a *characteristic polynomial* P:

$$P(z) = \sum_{r=0}^{R} g_r z^r = g_R \prod_{r=1}^{R} (z - z_r) \tag{12}$$

where the $\{z_r = \exp(\boldsymbol{i}\, k_r \Delta x)\}$ are, as in equation (7), the signal poles. The two expressions below show that these signal poles are the roots of the z-transform of $\boldsymbol{g}$, or equivalently that the wavenumbers $\{k_r\}$ are the roots of the Laplace transform of $\boldsymbol{g}$. The vanishing convolution between $\boldsymbol{s}$ and $\boldsymbol{g}$ can be expressed as a system of homogeneous equations using, once again, an Hankel matrix $\mathbf{H}$ of size $M \times R$:

$$\mathbf{H} \cdot \boldsymbol{g} = \mathbf{0} \tag{13}$$

and provides a way to estimate $\boldsymbol{g}$ from a measured signal either by (i) Ordinary Least-Squares (OLS) assuming that $g_0 = 0$ or (ii) Total Least-Squares (TLS) that identify $\boldsymbol{g}$ as the eigenvector $\boldsymbol{w}_\perp$ associated to the smaller eigenvalue $\lambda_\perp$ of the covariance matrix $\mathbf{C}_{ss}$ in equation (8).

This signal *deconvolution* technique has been widely studied in the system identification community [30], where it is applied to time data. In this 1D case, the equivalence between the plane wave decomposition (4) and zero-convolution kernel (13) is well established; moreover, the roots $\{z_r\}$ of the 1D kernel $\boldsymbol{g}$ can be estimated directly using the *companion matrix* of $P(z)$ (12) [31].

Recently, the INCOME algorithm (INverse COrrelation MEthod) [18] proposed to apply this method to multidimensional measurements using a TLS identification. In this case, the plane wave - zero kernel equivalence breaks: for example, a circular wave signal (e.g ponctual bending source in an isotropic thin plate) could fullfill the equation (13) with a small-order kernel $\boldsymbol{g}$, while needing an infinite number of plane wave components to be approximated by (4). As a consequence, the kernel identification method is able to give an unbiased estimate of the wave attenuation part, even for multidimensional signals. Moreover, the corresponding *multivariate* polynomial $P(z_1, \ldots, z_D)$ (with D the kernel dimension) is still an implicit definition of the structure's dispersion surfaces, that are the *affine varieties* of P (locations of its zeros) in $\mathbb{C}^D$. While the kernel estimation procedure is very simple to implement, determining the dispersion surfaces from $\boldsymbol{g}$ is in fact the hardest part, and involve some multidimensional complex root-finding schemes (or affine variety determination). In addition, the determination of $\boldsymbol{g}$ as the first eigenvector of the orthogonal subspace $\mathbf{W}_\perp$ makes it highly sensitive to noise.

4 Numerical comparison

4.1 Noise Sensitivity

The noise sensitivity of each aforementioned wavenumber estimation methods is investigated here using an elementary uni-dimensional signal model (4) with a single component ($R = 1$) and a reduced number of samples $N = 10$. The variance of the wavenumber estimations is computed using 1000 Monte-Carlo random sampling of an additive noise corresponding to a signal to noise ratio (SNR) of 10^3. In order to make the results more general, the obtained variances are compared to the Cramer-Rao Bound (CRB) of this particular signal model [32]. In particular, when the wavenumber is *purely* real (zero wave attenuation), the CRB is equal to:

$$\mathrm{CRB}_0 = \frac{12}{\mathrm{SNR} \times N^3} \tag{14}$$

Which shows that the wavenumber estimation should not be sensitive to its real part. This can be clearly observed in the figure 4a, where the normalized variance $\mathrm{var}(k)\,/\mathrm{CRB}_0$ is shown, for reach method, as a contour plot in the $z = \exp(\boldsymbol{i}\, k)$ plane, and demonstrates that the results are invariant with $\mathbb{R}\mathrm{e}\{k\} = \arg(z)$. The figure 4b thus focuses on the line $\mathbb{R}\mathrm{e}\{k\} = 0$ to show the effect of wave attenuation in the estimation variance. It can be observed that both Non-Linear Fit and ESPRIT methods are optimal in the sense that they provide estimates with variances on the lower Cramer-Rao Bound. By contrast, the Kernel-based estimation

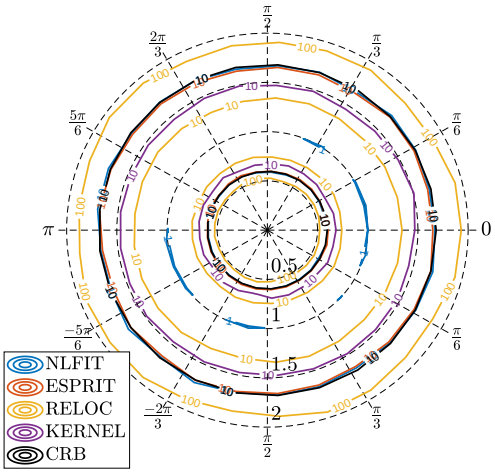

(a) Polar contour plot in the $z = \exp(\boldsymbol{i}\, k)$ plane

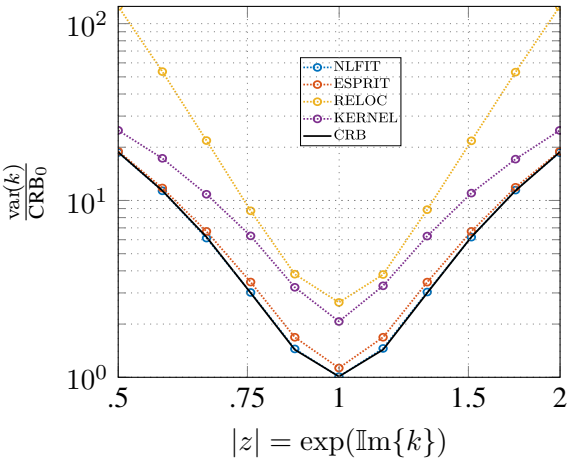

(b) Variance of the wavenumber estimation as a function of the wave attenuation, on the line $\mathbb{R}\mathrm{e}\{k\} = 0$

Figure 4: Variance of the wavenumber estimation normalized by the zero-attenuation Cramer-Rao Bound CRB_0 (14), for a model (4) with $R = 1$ and $N = 10$.

is characterized by a high variance (with a factor close to 2); this is due to the sensitivity of the least-significant eigenvectors of the signal covariance matrix with regard to noise. The least optimal method seems to be, in this particular situation, the spectrum relocalization method (RELOC); this can be related to the loss of signal model accuracy and data length associated to the pre-filtering technique.

4.2 Bias

The application of wavevector extraction methods on a multidimensional signal is submitted to *systematic* error, as the approximation of the measured kinematic response by a sum of waves (with a multidimensional version of the signal model (4)) is not exact, by contrast to the 1D case.

To demonstrate the consequence of such a biased approximation, this second numerical study considers the case of a free harmonic response corresponding to an isotropic Helholtz operator:

$$\mathscr{L}(u) = \frac{\partial u(\underline{\boldsymbol{x}})}{\partial x_1} + \frac{\partial u(\underline{\boldsymbol{x}})}{\partial x_2} + k^2\, u(\underline{\boldsymbol{x}}) = 0 \tag{15}$$

which, associated to a point source at $\underline{\boldsymbol{x}}_0$, generate a response $u(\underline{\boldsymbol{x}}) \propto \mathbb{J}_0(k\,\|\underline{\boldsymbol{x}} - \underline{\boldsymbol{x}}_0\|)$, where $\mathbb{J}_0$ is the Bessel function of the first kind.

The result of the analysis is shown on the figure 5, where the relative errors associated to the real part κ and the decay factor γ in the estimation of the wavenumber $k = \kappa(1 - \boldsymbol{i}\,\gamma) = \frac{6\pi}{L}(1 - 0.05\,\boldsymbol{i})$ are given as a function of the distance d to the source $\underline{\boldsymbol{x}}_0$. It can be observed that all methods based on a plane wave approximation (4) (NLFIT, ESRRIT and RELOC) provide poor estimates of the spatial decay γ (dashed lines), that is highly influenced by the geometrical decay and the cylindrical wavefront geometry. As the distance to the source increase, the far-field wavefront straightens thus the estimation error decreases. This model *bias* has a smaller influence on the real part of the wavenumber κ, which corresponding estimation error quickly decreases with the distance to the source.

By contrast to plane-wave expansion methods, the KERNEL-based identification provides extremely good estimations of both real and imaginary parts of the wavenumber (purple curves in the figure 5). Indeed, no plane wave assumption is involved in this method; instead, the equation (13) is used to estimate the

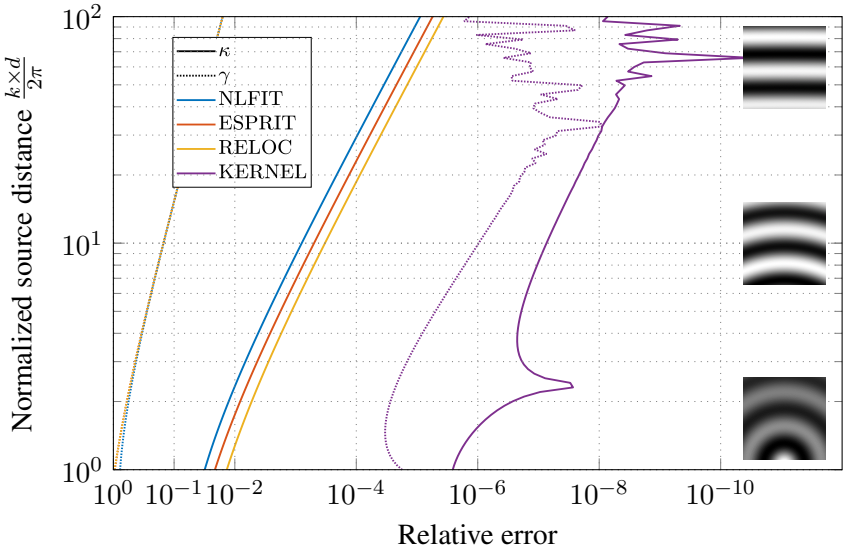

Figure 5: Wavevector estimation bias associated to cylindrical wave field. Effect of the distance d to the source $\underline{\boldsymbol{x}}_0$ in the estimation of the isotropic wavenumber $k = \kappa(1 - \boldsymbol{i}\,\gamma) = \frac{6\pi}{L}(1 - 0.05\,\boldsymbol{i})$.

coefficients (a, b, c) of a symmetric kernel $\mathbf{G} \in \mathbb{C}^{3\times 3}$ with the following shape:

$$\mathbf{G} = \begin{bmatrix} c & b & c \\ b & a & b \\ c & b & c \end{bmatrix} \tag{16}$$

that corresponds to a discrete version of the operator $\mathscr{L}$ in (15). The wavenumber is then estimated as the root of the Fourier transform of $\mathbf{G}$ that is closest to the real plane. Even in the absence of noise, the wavenumber estimation given by the KERNEL-based method is *not* exact; this can be related to two aspects: (i) in the near-field regime (close distnace to the source), the intrinsic *dispersion* of the chosen kernel which associated affine variety (locii of the roots of the Fourier transform) is not perfectly isotropic; (ii) in the far-field regime, the signal invariance along the wavefront plane making the estimation (13) badly conditioned, producing the error oscillations that can be observed on the figure 5.

5 Conclusions

In this communication, the use of dispersion surfaces as an intermediate step to structure identification is motivated throughout experimental examples. Then, a number of available approaches are presented, allowing to increase the wavevector resolution when few wavelengths are contained in the signal and/or an estimation the spatial wave decay is needed. Finally, the performance of all methods is compared with two numerical examples, giving insights on the sensitivities of the estimates to noise and signal modeling errors.

Despite its rather simplicity of implementation, the non-linear fitting technique (NLFIT) is limited to elementary cases (e.g when only one wave is present in the signal or when the different wavenumbers are related with in a known sequence). Thus the use of the more general ESPRIT method, that provides a closed-form estimate of the wavevectors, is advised when the measured signal can be well approximated by a relatively reduced number of plane waves: in one-dimensional signals, or for multidimensional structures in the far-field regime. In order to increase the maximum signal order that can be estimated with ESPRIT-type approaches, a spectrum RELOCalization technique was presented. However, the influence of the chosen window function on the obtained estimates is still to be investigated. Finally the KERNEL-based approach seems to be a very good candidate for the identification of dispersion surfaces of multidimensional structures. However, its high sensitivity to noise limits for now its application to experimental signals.

References

[1] J. Baqersad, P. Poozesh, C. Niezrecki, and P. Avitabile, "Photogrammetry and optical methods in structural dynamics–a review," Mechanical Systems and Signal Processing, vol. 86, pp. 17–34, 2017.

[2] S. Avril, M. Bonnet, A.-S. Bretelle, M. Grédiac, F. Hild, P. Ienny, F. Latourte, D. Lemosse, S. Pagano, E. Pagnacco et al., "Overview of identification methods of mechanical parameters based on full-field measurements," Experimental Mechanics, vol. 48, no. 4, pp. 381–402, 2008.

[3] E. Reynders, "System identification methods for (operational) modal analysis: review and comparison," Archives of Computational Methods in Engineering, vol. 19, no. 1, pp. 51–124, 2012.

[4] D. Chimenti, "Review of air-coupled ultrasonic materials characterization," Ultrasonics, vol. 54, no. 7, pp. 1804–1816, 2014.

[5] C. Pezerat and J. Guyader, "Identification of vibration sources," Applied acoustics, vol. 61, no. 3, pp. 309–324, 2000.

[6] Q. Leclère, F. Ablitzer, and C. Pézerat, "Practical implementation of the corrected force analysis technique to identify the structural parameter and load distributions," Journal of Sound and Vibration, vol. 351, pp. 106–118, 2015.

[7] F. Marchetti, K. Ege, and Q. Leclere, "Development of the corrected force analysis technique for laminated composite panels," Journal of Sound and Vibration, vol. 490, p. 115692, 2021.

[8] F. Pierron and M. Grédiac, The virtual fields method: extracting constitutive mechanical parameters from full-field deformation measurements. Springer Science & Business Media, 2012.

[9] A. Berry, O. Robin, and F. Pierron, "Identification of dynamic loading on a bending plate using the virtual fields method," Journal of Sound and Vibration, vol. 333, no. 26, pp. 7151–7164, 2014.

[10] J. Cuenca, F. Gautier, and L. Simon, "Measurement of complex bending stiffness of a flat panel covered with a viscoelastic layer using the image source method," in 8th European Conference on Noise Control, 2009.

[11] F. Marchetti, N. B. Roozen, J. Segers, K. Ege, M. Kersemans, and Q. Leclere, "Experimental methodology to assess the dynamic equivalent stiffness properties of elliptical orthotropic plates," Journal of Sound and Vibration, vol. 495, p. 115897, 2021.

[12] N. Ferguson, C. Halkyard, B. Mace, and K. Heron, "The estimation of wavenumbers in two-dimensional structures," in Proceedings of ISMA, vol. 2, 2002, pp. 799–806.

[13] J. Berthaut, M. Ichchou, and L. Jezequel, "K-space identification of apparent structural behaviour," Journal of Sound and Vibration, vol. 280, no. 3-5, pp. 1125–1131, 2005.

[14] R. Cherif, J.-D. Chazot, and N. Atalla, "Damping loss factor estimation of two-dimensional orthotropic structures from a displacement field measurement," Journal of sound and vibration, vol. 356, pp. 61–71, 2015.

[15] A. Geslain, S. Raetz, M. Hiraiwa, M. Abi Ghanem, S. Wallen, A. Khanolkar, N. Boechler, J. Laurent, C. Prada, A. Duclos et al., "Spatial laplace transform for complex wavenumber recovery and its application to the analysis of attenuation in acoustic systems," Journal of Applied Physics, vol. 120, no. 13, p. 135107, 2016.

[16] P. Margerit, A. Lebée, J.-F. Caron, and X. Boutillon, "High resolution wavenumber analysis (hrwa) for the mechanical characterisation of viscoelastic beams," Journal of Sound and Vibration, vol. 433, pp. 198–211, 2018.

[17] P. Margerit, A. Lebée, J.-F. Caron, K. Ege, and X. Boutillon, "The high-resolution wavevector analysis for the characterization of the dynamic response of composite plates," Journal of Sound and Vibration, vol. 458, pp. 177–196, 2019.

[18] R. F. Boukadia, C. Claeys, C. Droz, M. Ichchou, W. Desmet, and E. Deckers, "An inverse convolution method for wavenumber extraction (income): Formulations and applications," Journal of Sound and Vibration, vol. 520, p. 116586, 2022.

[19] I. Bartoli, A. Marzani, F. L. Di Scalea, and E. Viola, "Modeling wave propagation in damped waveguides of arbitrary cross-section," Journal of sound and vibration, vol. 295, no. 3-5, pp. 685–707, 2006.

[20] J. G. McDaniel and W. S. Shepard Jr, "Estimation of structural wave numbers from spatially sparse response measurements," The Journal of the Acoustical Society of America, vol. 108, no. 4, pp. 1674–1682, 2000.

[21] R. Schmidt, "Multiple emitter location and signal parameter estimation," IEEE transactions on antennas and propagation, vol. 34, no. 3, pp. 276–280, 1986.

[22] Y. Hua and T. K. Sarkar, "Matrix pencil method for estimating parameters of exponentially damped/undamped sinusoids in noise," IEEE Transactions on Acoustics, Speech, and Signal Processing, vol. 38, no. 5, pp. 814–824, 1990.

[23] R. Roy and T. Kailath, "Esprit-estimation of signal parameters via rotational invariance techniques," IEEE Transactions on acoustics, speech, and signal processing, vol. 37, no. 7, pp. 984–995, 1989.

[24] P. D. Grünwald, The minimum description length principle. MIT press, 2007.

[25] R. Badeau, B. David, and G. Richard, "A new perturbation analysis for signal enumeration in rotational invariance techniques," IEEE Transactions on Signal Processing, vol. 54, no. 2, pp. 450–458, 2006.

[26] J.-M. Papy, L. De Lathauwer, and S. Van Huffel, "A shift invariance-based order-selection technique for exponential data modelling," IEEE signal processing letters, vol. 14, no. 7, pp. 473–476, 2007.

[27] K. Ege, X. Boutillon, and B. David, "High-resolution modal analysis," Journal of sound and vibration, vol. 325, no. 4-5, pp. 852–869, 2009.

[28] S. A. Fulop and K. Fitz, "Algorithms for computing the time-corrected instantaneous frequency (reassigned) spectrogram, with applications," The Journal of the Acoustical Society of America, vol. 119, no. 1, pp. 360–371, 2006.

[29] R. Prony, "Essai experimental et analytique," J. de l'Ecole Polytechnique, vol. 2, p. 929, 1795.

[30] I. Markovsky, Low rank approximation: algorithms, implementation, applications. Springer, 2012, vol. 906.

[31] A. Edelman and H. Murakami, "Polynomial roots from companion matrix eigenvalues," Mathematics of Computation, vol. 64, no. 210, pp. 763–776, 1995.

[32] R. Kumaresan and D. Tufts, "Estimating the parameters of exponentially damped sinusoids and pole-zero modeling in noise," IEEE transactions on acoustics, speech, and signal processing, vol. 30, no. 6, pp. 833–840, 1982.